

Speckle Reduction with Adaptive Stack Filters

María Elena Buemi*

Departamento de Computación, Facultad de Ciencias Exactas y Naturales, Universidad de Buenos Aires, Pabellón I, Argentina

Alejandro C. Frery, Heitor S. Ramos

LCCV & LaCCAN/CPMAT, Universidade Federal de Alagoas, BR 104 Norte km 97, 57072-970 Maceió, AL – Brazil

Abstract

Stack filters are a special case of non-linear filters. They have a good performance for filtering images with different types of noise while preserving edges and details. A stack filter decomposes an input image into stacks of binary images according to a set of thresholds. Each binary image is then filtered by a Boolean function, which characterizes the filter. Adaptive stack filters can be computed by training using a prototype (ideal) image and its corrupted version, leading to optimized filters with respect to a loss function. In this work we propose the use of training with selected samples for the estimation of the optimal Boolean function. We study the performance of adaptive stack filters when they are applied to speckled imagery, in particular to Synthetic Aperture Radar (SAR) images. This is done by evaluating the quality of the filtered images through the use of suitable image quality indexes and by measuring the classification accuracy of the resulting images. We used SAR images as input, since they are affected by speckle noise that makes classification a difficult task.

Keywords: Non-linear filters, speckle noise, stack filters, SAR image filtering

*Corresponding author. Fax: +54 11 4576 3359
Email address: `mebuemi@dc.uba.ar` (María Elena Buemi)

1. Introduction

SAR images are generated by a coherent illumination system and are affected by the coherent interference of the signal from the terrain (Oliver and Quegan, 1998). This interference causes fluctuations of the detected intensity which varies from pixel to pixel, an effect called speckle noise, that also appears in ultrasound-B, laser and sonar imagery.

Speckle noise, unlike noise in optical images, is neither Gaussian nor additive; it follows other distributions and is multiplicative. Classical techniques, therefore, lead to suboptimal results when applied to this kind of imagery. Among the authors that have studied the problem of adapting classical image processing methods to SAR data, Lee (1981) provides a good starting point.

The physics of image formation leads to the following model: the observed data can be described by the random field Z , defined as the product of two independent random fields: X , the backscatter, and Y , the speckle noise.

The backscatter is a physical magnitude that depends on the geometry and water content of the surface being imaged, as well as on the angle of incidence, frequency and polarization of the electromagnetic radiation emitted by the radar. It is the main source of information sought in SAR data.

Speckle has a major impact on the accuracy of classification procedures (Mejail et al., 2003; Capstick and Harris, 2001), since it introduces a low signal-to-noise ratio. The effectiveness of techniques for reducing speckle can be measured, among other quantities (see Moschetti et al., 2006, for instance), through the accuracy of simple classification methods. The most widespread statistical classification technique is Gaussian maximum likelihood.

Different statistical distributions have been proposed in the literature for describing speckled data. Gao (2010) presents a comprehensive and updated survey of univariate distributions able to describe speckled data. In this work, since we are dealing with intensity format, we use the Gamma distribution, denoted by Γ , for the speckle, and the reciprocal of Gamma distribution, denoted by Γ^{-1} , for the backscatter. These assumptions, and the independence between

31 the fields, result in the intensity \mathcal{G}^0 law for the return (Frery et al., 1997; Me-
32 jail et al., 2003). This family of distributions is indexed by three parameters:
33 roughness α , scale γ , and the number of looks L , and it has been validated as an
34 universal model for several types of targets. Intensity data is obtained by sum-
35 ming the squared real and imaginary parts of the complex return; Vasconcellos
36 et al. (2005) discuss properties of this type of speckled data.

37 Stack filters are a special case of non-linear filters. They have good perfor-
38 mance for improving images with different types of noise while preserving edges
39 and details. Various authors have studied these filters, and many methods have
40 been developed for their construction and applicaton (Prasad, 2005; Shi et al.,
41 2005).

42 These filters decompose the input image, by thresholds, in binary slices form-
43 ing a stack of data. Each binary image is then filtered using a Boolean function
44 evaluated on a sliding window. The resulting image is obtained summing up all
45 the filtered binary images. The application of stack filters to speckled data was
46 studied by Buemi et al. (2007, 2011).

47 The main drawback of using stack filters is the need to compute the Boolean
48 functions that satisfy a certain criterion. Direct computation on the set of all
49 Boolean functions is unfeasible, and promising techniques rely on a learning
50 procedure: the use of a pair of images, namely the ideal and corrupted one,
51 and of a loss function. The Boolean functions are sought to provide the best
52 estimator of the former using the latter as input. The stack filter design method
53 used in this work is based on an algorithm proposed by Yoo et al. (1999). The
54 drawback of this line of action is the need of a pure, noiseless image.

55 Finn et al. (2011) provide a comprehensive and updated review of the liter-
56 ature on speckle filters, with a view towards echocardiographic imagery. They
57 propose a categorization, within which our proposal should be included in the
58 “SAR” category.

59 We propose the use of user-provided information. The user selects as many
60 regions of interest as desired, and after a descriptive and quantitative analysis
61 of the data, he/she provides an “ideal” value for each region. The Boolean

62 functions are then sought to provide an estimator of such values in the cor-
 63 responding areas. This approach reduces the computational effort of building
 64 the Boolean functions and, at the same time, gives the option of providing a
 65 noiseless complete image or specifying “ideal” values in regions chosen by the
 66 user.

67 We study the application of this type of filter to SAR images, assessing its
 68 performance by evaluating the quality of the filtered images through the use of
 69 objective image quality indexes like the universal image quality index and the
 70 correlation measure index and by measuring the classification accuracy of the
 71 resulting images using maximum likelihood Gaussian classification.

72 The structure of this paper is as follows. Section 2 summarizes the \mathcal{G}^0 model
 73 for speckled data. Section 3 reviews stack filters, and describes the filter design
 74 method used in this work. In Section 4 we discuss the results of filtering through
 75 image quality assessment and classification performance. Finally, in Section 5
 76 we present the conclusions.

77 2. The Multiplicative Model

78 Following Moschetti et al. (2006), we will only present the univariate inten-
 79 sity case. Other formats (amplitude and complex) are treated in detail in Frery
 80 et al. (1997).

The intensity \mathcal{G}^0 distribution that describes speckled return Z is character-
 ized by the following density:

$$f(z) = \frac{n^n \Gamma(n - \alpha)}{\gamma^\alpha \Gamma(n) \Gamma(-\alpha)} \frac{z^{n-1}}{(\gamma + nz)^{n-\alpha}},$$

81 where $-\alpha, \gamma, z > 0, n \geq 1$. This situation is denoted $Z \sim \mathcal{G}^0(\alpha, \gamma, n)$.

82 The α parameter describes the image roughness or texture. It adopts neg-
 83 ative values, varying from $-\infty$ to 0. If α is near 0, then the image data are
 84 extremely rough (for example: urban areas), and if α is far from the origin
 85 then the data correspond to a smooth region (for example: pasture areas). The
 86 values for forests lay in-between.

87 The r -th order moment of a $\mathcal{G}^0(\alpha, \gamma, n)$ -distributed random variable is given
 88 by

$$E(Z^r) = \left(\frac{\gamma}{n}\right)^r \frac{\Gamma(-\alpha - r)\Gamma(n + r)}{\Gamma(-\alpha)\Gamma(n)}, \quad (1)$$

89 if $-n > \alpha$ and infinite if otherwise.

90 Many filters have been proposed in the literature for reducing speckle noise,
 91 among them the ones by Lee (1986), by Kuan et al. (1987) and by Frost et al.
 92 (1982). These filters will be applied to speckled data, along with the filter
 93 proposed in this work. For quality performance the comparison will be done
 94 between the results of applying the stack filter and the Lee filter, since the
 95 latter is considered one of the touchstones for speckle reduction. Classification
 96 performance will be assessed by classifying data filtered with the Lee, Frost and
 97 stack filters using Gaussian maximum likelihood. The two first filters can be
 98 considered classical choices in the area.

99 3. Stack Filters

100 This section is dedicated to a brief synthesis of stack filter definitions and
 101 design. For more details on this subject, the reader is referred to the works by
 102 Astola and Kuosmanen (1997); Lin and Kim (1994); Yoo et al. (1999).

Consider images of the form $X: S \rightarrow \{0, \dots, M\}$, with S the support and
 $\{0, \dots, M\}$ the set of admissible values. The threshold is the set of operators
 $T^m: \{0, \dots, M\} \rightarrow \{0, 1\}$ given by

$$T^m(x) = \begin{cases} 1 & \text{if } x \geq m, \\ 0 & \text{if } x < m. \end{cases}$$

103 We will use the notation $X^m = T^m(x)$. According to this definition, the value
 104 of a non-negative integer number $x \in \{0, \dots, M\}$ can be reconstructed making
 105 the summation of its thresholded values between 0 and M .

106 In the following, we show an example of the threshold decomposition of an
 107 unidimensional signal. Let $X = [2, 1, 3, 2, 3]$ be a signal. Its decomposition is
 108 given by: $X^1 = [1, 1, 1, 1, 1]$, $X^2 = [1, 0, 1, 1, 1]$, $X^3 = [0, 0, 1, 0, 1]$.

109 Let $X = (x_0, \dots, x_{n-1})$ and $Y = (y_0, \dots, y_{n-1})$ be binary vectors of length
 110 n . Define an order relation given by $X \leq Y$ if and only if $x_i \leq y_i$ holds true
 111 for every i . This relation is reflexive, anti-symmetric and transitive, generating
 112 therefore a partial ordering on the set of binary vectors of fixed length.

A Boolean function $f: \{0, 1\}^n \rightarrow \{0, 1\}$, where n is the length of the input
 vectors, has the stacking property if and only if

$$\forall X, Y \in \{0, 1\}^n, X \leq Y \Rightarrow f(X) \leq f(Y).$$

113 We say that f is a positive Boolean function if and only if it can be written
 114 by means of an expression that contains only non-complemented input variables.
 115 That is,

$$f(x_1, x_2, \dots, x_n) = \bigvee_{i=1}^K \bigwedge_{j \in P_i} x_j, \quad (2)$$

116 where n is the number of arguments of the function, K is the number of terms of
 117 the expression and P_i is a subset of the interval $\{1, \dots, N\}$, ‘ \vee ’ and ‘ \wedge ’ denote,
 118 respectively, the AND and OR Boolean operators. It is possible to prove that
 119 this type of functions has the stacking property.

A stack filter is defined by the function $S_f: \{0, \dots, M\}^n \rightarrow \{0, \dots, M\}$,
 corresponding to the Positive Boolean function $f(x_1, x_2, \dots, x_n)$ expressed in
 the form given in equation (2). The function S_f can be expressed by means of
 a summation:

$$S_f(X) = \sum_{m=1}^M f(T^m(X)).$$

120 In this work we applied the stack filter generated with the fast algorithm
 121 described in Lin et al. (1990); Lin and Kim (1994); Yoo et al. (1999).

122 Stack filters are built by a training process that generates a positive Boolean
 123 function that preserves the stacking property. Originally, this training is per-
 124 formed providing two complete images on S , one degraded and one noiseless.
 125 The algorithm seeks the operator that best estimates the later using the former
 126 as input, with respect to a loss function.

127 The implementation developed for this work supports the application of the
 128 stack filter many times. Our approach consists of using, instead of that pair of

129 images, a set of regions of interest, much smaller than the whole data set, and
 130 relying on the analysis the user makes of this information. Besides not needing
 131 a noiseless image, the user is free to impose its prior knowledge and assumptions
 132 on the resulting image.

133 The performance of the proposed filters is assessed both by qualitative and
 134 quantitative analyses. The system has an interface which shows the user the
 135 mean value of each region, and suggests it as the default “desired” value, but
 136 he/she can choose other from a menu (including the median, the lower and upper
 137 quartiles and a free specification). This freedom of choice is particularly useful
 138 when dealing with non-Gaussian degradation as is the case of, for instance,
 139 impulsive noise.

140 4. Results

141 In this section, we present the results of building stack filters by the afore-
 142 mentioned training. These filters are applied to both simulated and real data.
 143 The quality of the results is assessed in two different manners: one using image
 144 quality objective measures, and other evaluating the influence of filtering on
 145 maximum likelihood classification.

146 4.1. Image quality indexes

147 The indexes used to evaluate the quality of the filtered images are the uni-
 148 versal image quality index Wang and Bovik (2002) and the correlation measure
 149 β . The universal image quality index Q is given by equation (3)

$$Q = \frac{\sigma_{XY}}{\sigma_X \sigma_Y} \frac{2\bar{X}\bar{Y}}{\bar{X}^2 + \bar{Y}^2} \frac{2\sigma_X \sigma_Y}{\sigma_X^2 + \sigma_Y^2}, \quad (3)$$

150 where $\sigma_X^2 = (N - 1)^{-1} \sum_{i=1}^N (X_i - \bar{X})^2$, $\sigma_Y^2 = (N - 1)^{-1} \sum_{i=1}^N (Y_i - \bar{Y})^2$, $\bar{X} =$
 151 $N^{-1} \sum_{i=1}^N X_i$ and $\bar{Y} = N^{-1} \sum_{i=1}^N Y_i$. The dynamic range of index Q is $[-1, 1]$,
 152 being 1 the best value. To evaluate the index of the whole image, local indexes
 153 Q_i are calculated for each pixel using a suitable square window, and then these

154 results are averaged to yield the total image quality Q . The correlation measure
 155 is given by equation (4)

$$\beta = \frac{\sigma_{\nabla^2 X \nabla^2 Y}}{\sigma_{\nabla^2 X}^2 \sigma_{\nabla^2 Y}^2}, \quad (4)$$

156 where $\nabla^2 X$ and $\nabla^2 Y$ are the Laplacians of images X and Y , respectively. The
 157 correlation measure range is $[-1, 1]$.

158 4.2. Observed metrics

159 A Monte Carlo experiment was performed, generating 1000 independent
 160 replications of synthetic 1-look SAR images for each of four contrast ratios.
 161 The generated images consist of two regions separated by a vertical straight
 162 border. Each sample corresponds to a different contrast ratio, which ranges
 163 from 10:1 to 10:8. This was done in order to study the effect of the contrast
 164 ratio in the quality indexes considered.

165 Table 1 shows the mean correlation measure β and the mean quality index Q ,
 166 as computed in the Monte Carlo experiment. The comparison is made between
 167 Lee filtered and stack filtered SAR images.

168 It can be seen that, according to the results obtained for the β index, the
 169 stack filter exhibits a better performance at high contrast ratios, namely 10:1
 170 and 10:2, while the Lee filter shows the opposite behavior. The results for the Q
 171 index show slightly better results for the stack filter all over the range of contrast
 172 ratios. It is remarkable the small variance of these estimations, compared to the
 173 mean values obtained.

174 Figure 1 shows the boxplots of the observations summarized in Table 1.
 175 From the plots for the β index, it can be seen that, the Lee filter has a lower
 176 degree of variability with contrast and that both are almost symmetric. The
 177 plots of the Q index show a better performance for the stack filter for all the
 178 contrast ratios considered.

179 The image resulting of applying the stack filter 95 times and the image
 180 produced by the application of the Lee filter. This was found the ideal number
 181 of iterations for this study: less iterations produced images with visible noise,
 182 while more iterations introduced blurring. An automatic stopping criterion is a

Table 1: Statistics from image quality indexes

β index				
	Stack filter		Lee filter	
contrast	$\bar{\beta}$	s_{β}	$\bar{\beta}$	s_{β}
10 : 1	0.1245	0.0156	0.0833	0.0086
10 : 2	0.0964	0.0151	0.0663	0.0079
10 : 4	0.0267	0.0119	0.0421	0.0064
10 : 8	-0.0008	0.0099	0.0124	0.0064
Q index				
	Stack filter		Lee filter	
contrast	\bar{Q}	s_Q	\bar{Q}	s_Q
10 : 1	0.0159	0.0005	0.0156	0.0004
10 : 2	0.0154	0.0005	0.0148	0.0004
10 : 4	0.0124	0.0008	0.0120	0.0006
10 : 8	0.0041	0.0013	0.0021	0.0006

183 venue for future research. The presented results are the mean values obtained
 184 from a Monte Carlo experiment involving different contrast ratios.

185 *4.3. Classification performance*

186 The equality of the classification results are obtained by calculating the
 187 confusion matrix, after Gaussian Maximum Likelihood Classification (GMLC).

188 Figure 2(a), left, presents an image 128×128 pixels, simulated with two
 189 regions: samples from the $\mathcal{G}^0(-1.5, \gamma_{-1.5,1}^*, 1)$ and from the $\mathcal{G}^0(-10, 10\gamma_{-10,1}^*, 1)$
 190 laws form the left and right halves, respectively, where $\gamma_{\alpha,n}^*$ denotes the scale
 191 parameter that, for a given roughness α and number of looks n yields an uni-
 192 tary mean law. In this manner, Figure 2(a) presents data that are hard to
 193 classify: extremely heterogeneous and homogeneous areas with the lowest pos-
 194 sible signal-to-noise ratio ($n = 1$). The mean value of the dashed area was used

195 as the “ideal” image. Figures 2(b) and 2(c), left, show the result of applying the
 196 resulting filter once and 95 times, respectively. The right side of Figures 2(a),
 197 2(b) and 2(c) present the GMLC of each image. Not only the pointwise im-
 198 provement is notorious, but the edge presevation is also noteworthy, specially
 199 in Figure 2(c), right, where the straight border has been completely retrieved.

200 Figure 3 compares the performance of the proposed stack filter with respect
 201 to two widely used SAR filters: Lee and Frost. Figure 3(a) presents the original
 202 data, and the regions of interest used for estimating the Boolean function; the
 203 data are from the ESAR sensor and show two distinct agricultural areas with
 204 possibly a raw of trees (the high return strip). The data are from the HV
 205 polarization, L-band with about $1\text{ m} \times 1.5\text{ m}$ pixel size and of $3\text{ m} \times 2.2\text{ m}$ spatial
 206 resolution. In this case, again, the mean on each region was used as the ‘ideal’
 207 image. Figures 3(b), 3(c), 3(d) and 3(e) present the result of applying the Frost,
 208 Lee and Stack filters (one and 22 iterations; this last choice, again, obtained by
 209 visual inspection) to the original SAR data. The right side of previous figures
 210 present the corresponding GMLC. The stack filter produces better results than
 211 classical despeckling techniques.

212 Table 2 presents the main results from the confusion matrices of all the
 213 GMLC, including the results presented in Buemi et al. (2007) which used the
 214 classical stack filter estimation with whole images. It shows the percentage of
 215 pixels that was labeled by the user as from region R_i that was correctly classified
 216 as belonging to region R_i , for $1 \leq i \leq 3$. “None” denotes the results on the
 217 original, unfiltered, data, “Sample Stack k ” denotes our proposal of building
 218 stack filters with samples, applied k times, “Stack k ” the classical construction
 219 applied k times, and “Frost” and “Lee” the classical speckle reduction filters. It
 220 is clear the superior performance of stack filters (both classical and by training)
 221 over speckle filters, though the stack filter by training requires more than a
 222 single iteration to outperform the last ones. Stack filters by training require
 223 about two orders of time less than classical stack filters to be built, and they
 224 produce comparable results. Using regions of interest is, therefore, a competitive
 225 approach for the definition of this kind of filters.

Table 2: Statistics from the confusion matrices

Filter	R_1/R_1	R_2/R_2	R_3/R_3
None	13.40	48.16	88.90
Sample Stack 1	9.38	65.00	93.19
Sample Stack 22	63.52	74.87	96.5
Stack 1	14.35	64.65	90.86
Stack 40	62.81	89.09	94.11
Stack 95	63.01	93.20	94.04
Frost	16.55	55.54	90.17
Lee	16.38	52.72	89.21

226 *4.4. Contrast preservation*

227 We use a second phantom of strips and points to assess contrast and edge
 228 preservation. It consists of an image of size 256×256 pixels with two regions:
 229 one formed by strips of several widths on a background. The data in the for-
 230 mer are distributed according to a $\mathcal{G}^0(\alpha_1, \gamma_{\alpha,1}^*, 1)$ law, and the latter obey a
 231 $\mathcal{G}^0(\alpha_2, \gamma_{\alpha,1}^*, 1)$ distribution, where $\gamma_{\alpha,n}^*$ is the scale, $\alpha \in \{-10, \dots, -1\}$ is the
 232 roughness parameter and the number of looks is held constant in the noisiest
 233 case, namely $n = 1$.

The factor used in this experiment was the contrast between light areas
 (strips and points) and background, measured as

$$\frac{|\mu_1 - \mu_2|}{\sqrt{\sigma_1^2 + \sigma_2^2}},$$

234 which considers the mean and the standard deviation of each region. These
 235 values, which depend on the three parameters of the \mathcal{G}^0 distribution can be
 236 computed using the expression of moments given in equation (1). Nascimento
 237 et al. (2010) present other contrast measures based on stochastic divergences
 238 between distributions.

239 An ideal filter reduces the noise without affecting the contrast. A blurry

240 filter will smudge the edges, mixing classes and reducing the contrast. Since
 241 the phantom presented in Figure 4(a) consists of thin light strips and isolated
 242 points on a dark background, the strips and points will tend to disappear if the
 243 filter introduces blur.

244 Table 3 presents the relative contrast error between the theoretical and ob-
 245 served values; the latter is the mean over one hundred replications.

Table 3: Relative contrast error introduced by the filters

α_1, α_2	Contrast	Stack	Lee	Frost
-1, -5	0.0033	0.0096	0.0094	0.0883
-2, -8	0.0033	0.0049	0.0093	0.2470
-6, -2	0.0034	0.0088	0.0097	0.2095

246 The Frost filter presents the best performance, but it also alters the contrast
 247 between regions as can be seen in Figure 4. The stack filter outperforms by a
 248 small margin the Lee filter in two out of three cases, but both are much better
 249 than the Frost filter regarding contrast preservation. Visual inspection confirms
 250 previous results: the stack filter is more effective at reducing speckle than the
 251 other two techniques, as can be seen in Figure 4.

252 5. Conclusions

253 In this work, the effect of adaptive stack filtering on SAR images was as-
 254 sessed. Two viewpoints were considered: a classification performance viewpoint
 255 and a quality perception viewpoint. For the first approach, the Frost and Lee
 256 filters were compared with the iterated stack filter using a metric extracted from
 257 the confusion matrix. A real SAR image was used in this case. For the second
 258 approach, a Monte Carlo experience was carried out in which 1-look synthetic
 259 SAR, i.e., the noisiest images, were generated. In this case, the Lee filter and a
 260 one pass stack filter were compared for various degrees of contrast. The β and
 261 the Q indexes were used as measures of perceptual quality. The results of the

262 β index shows that the stack filter performs better in cases of high contrast.
263 The results of the Q index show slightly better performance of the stack filter
264 over the Lee filter. This quality assessment is not conclusive but indicates the
265 potential of stack filters in SAR image processing for visual analysis. The clas-
266 sification results and the quality perception results suggest that stack filters are
267 promising tools in SAR image processing and analysis.

268 The results obtained using the contrast measure given by formula 4.4 show a
269 comparatively good performance of the stack Filter. The system was developed
270 in Matlab, and the code is available from the first author upon request.

271 **References**

272 Astola, J., Kuosmanen, P., 1997. Fundamentals of Nonlinear Digital Filtering.
273 CRC Press, Boca Raton.

274 Buemi, M. E., Mejail, M., Jacobo, J., Frery, A. C., Ramos, H. S., 2011. Assess-
275 ment of SAR image filtering using adaptive stack filters. In: Proceedings 16th
276 Iberoamerican Congress on Pattern Recognition (CIARP 2011). Vol. 7042 of
277 Lecture Notes in Computer Science. Springer, Pucón, Chile, pp. 89–96.

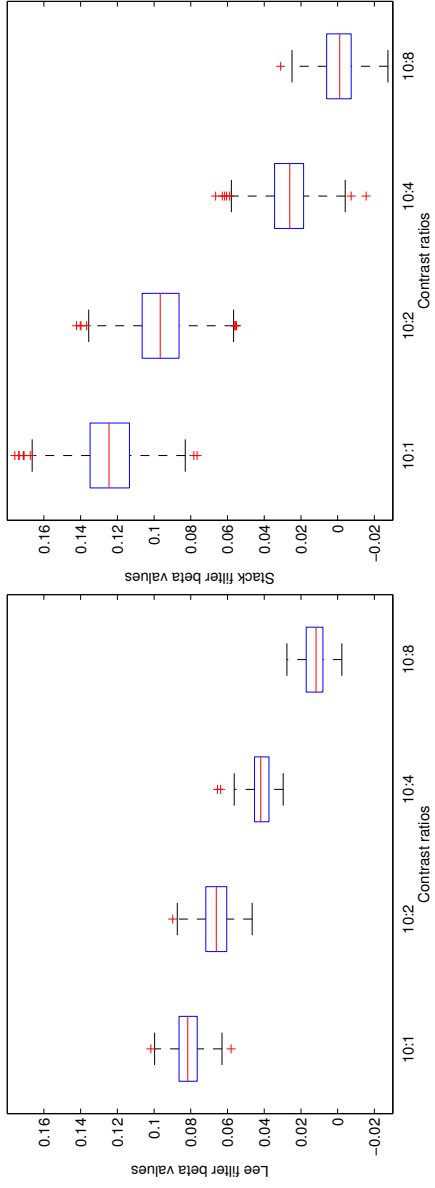
278 Buemi, M. E., Mejail, M. E., Jacobo-Berlles, J., Gambini, J., 2007. Improve-
279 ment in SAR image classification using adaptive stack filters. In: Proceedings
280 XX Brazilian Symposium on Computer Graphics and Image Processing (SIB-
281 GRAPI). IEEE Computer Press, pp. 263–270.

282 Capstick, D., Harris, R., Dec. 2001. The effects of speckle reduction on classi-
283 fication of ERS SAR data. International Journal of Remote Sensing 22 (18),
284 3627–3641.

285 Finn, S., Glavin, M., Jones, E., JAN 2011. Echocardiographic speckle reduction
286 comparison. IEEE Transactions on Ultrasonics Ferroelectrics and Frequency
287 Control 58 (1), 82–101.

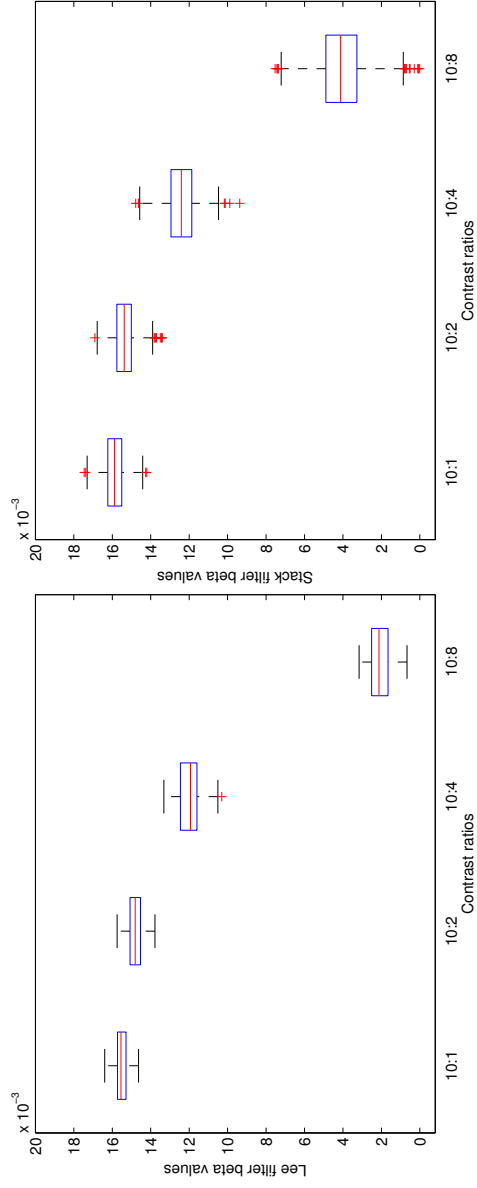
- 288 Frery, A. C., Müller, H.-J., Yanasse, C. C. F., Sant'Anna, S. J. S., 1997. A
289 model for extremely heterogeneous clutter. *IEEE Transactions on Geoscience*
290 *and Remote Sensing* 35 (3), 648–659.
- 291 Frost, V. S., Stiles, J. A., Shanmugan, K. S., Holtzman, J., 1982. A model for
292 radar images and its application to adaptive digital filtering of multiplica-
293 tive noise. *IEEE Transactions on Pattern Analysis and Machine Intelligence*
294 *PAMI-4* (2), 157–166.
- 295 Gao, G., 2010. Statistical modeling of SAR images: A survey. *Sensors* 10, 775–
296 795.
- 297 Kuan, D. T., Sawchuk, A. A., Strand, T. C., Chavel, P., March 1987. Adaptive
298 restoration of images with speckle. *IEEE Transactions on Acoustics Speech*
299 *and Signal Processing* 35 (3), 373–383.
- 300 Lee, J.-S., Apr. 1981. Refined filtering of image noise using local statistics.
301 *Computer Graphics and Image Processing* 15 (4), 380–389.
- 302 Lee, J. S., 1986. Speckle suppression and analysis for synthetic aperture radar
303 images. *Optical Engineering* 25, 636–643.
- 304 Lin, H.-J., Sellke, T. M., J.Coyle, E., June 1990. Adaptive stack filtering under
305 the mean absolute error criterion. *IEEE Transactions on Acoustics, Speech*
306 *and Signal Process* 38, 938–954.
- 307 Lin, J.-H., Kim, Y. T., 4 1994. Fast algorithms for training stack filters. *IEEE*
308 *Transactions on Signal Processing* 42 (3), 772–781.
- 309 Mejail, M. E., Jacobo-Berlles, J., Frery, A. C., Bustos, O. H., 2003. Classi-
310 fication of SAR images using a general and tractable multiplicative model.
311 *International Journal of Remote Sensing* 24 (18), 3565–3582.
- 312 Moschetti, E., Palacio, M. G., Picco, M., Bustos, O. H., Frery, A. C., 2006.
313 On the use of Lee's protocol for speckle-reducing techniques. *Latin American*
314 *Applied Research* 36 (2), 115–121.

- 315 Nascimento, A. D. C., Cintra, R. J., Frery, A. C., 2010. Hypothesis testing in
316 speckled data with stochastic distances. *IEEE Transactions on Geoscience*
317 *and Remote Sensing* 48 (1), 373–385.
- 318 Oliver, C., Quegan, S., 1998. *Understanding Synthetic Aperture Radar Images*.
319 Artech House.
- 320 Prasad, M. K., Mar 2005. Stack filter design using selection probabilities. *IEEE*
321 *Transactions on Signal Processing* 53 (3), 1025–1037.
- 322 Shi, G., Dong, W., Liu, Z., 7-10 Aug. 2005. Design and implementation of stack
323 filter based on immune memory clonal algorithms with hybrid computation.
324 In: *48th Midwest Symposium on Circuits and Systems*. pp. 1159–1162Vol.2.
- 325 Vasconcellos, K. L. P., Frery, A. C., Silva, L. B., 2005. Improving estimation in
326 speckled imagery. *Computational Statistics* 20 (3), 503–519.
- 327 Wang, Z., Bovik, A., mar 2002. A universal image quality index. *Signal Pro-*
328 *cessing Letters, IEEE* 9 (3), 81 –84.
- 329 Yoo, J., Fong, K. L., Huang, J.-J., Coyle, E. J., Adams III, G. B., 8 1999. A fast
330 algorithm for designing stack filters. *IEEE Transactions on Image Processing*
331 8 (8), 772–781.



(a) Values of β , Lee filter

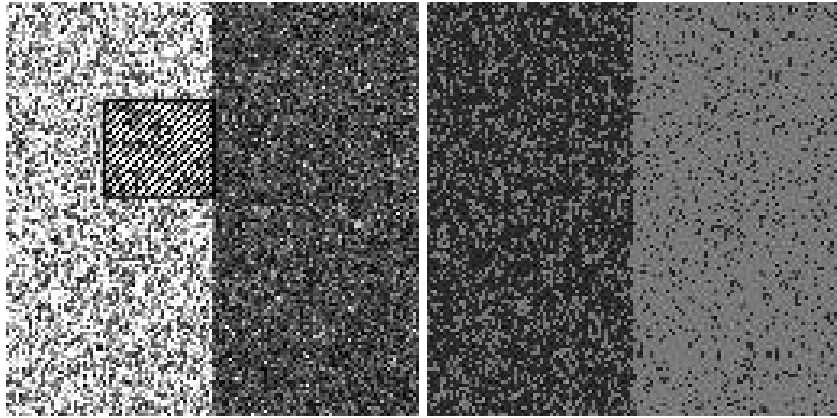
(b) Values of β , Stack filter



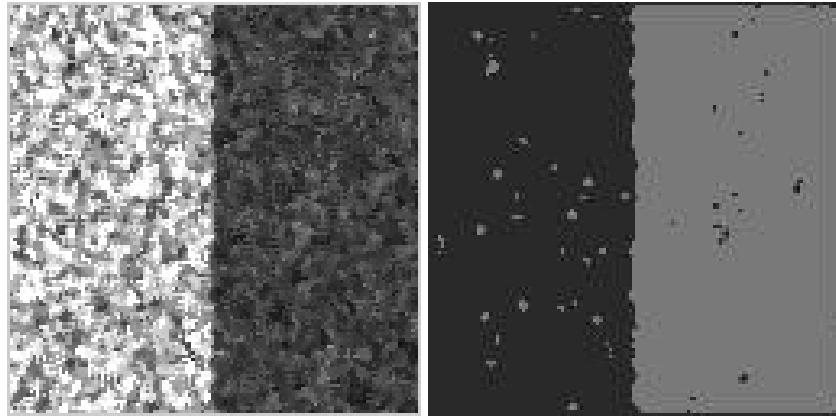
(c) Lee filter values of Q

(d) Stack filter values of Q

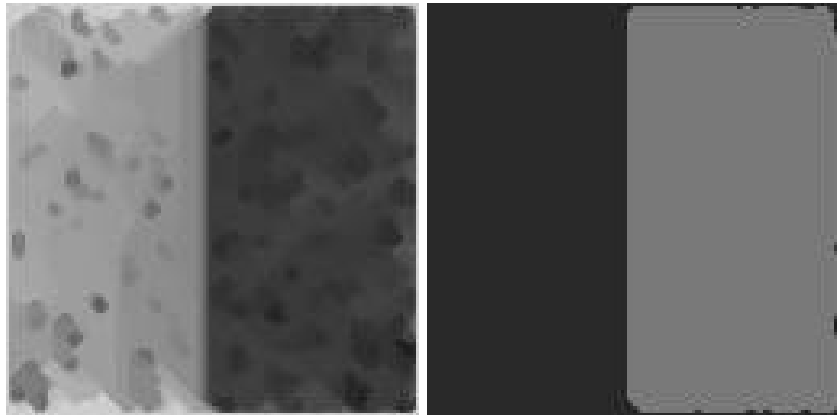
Figure 1: Boxplots of the quality indexes



(a) Simulated image and GMLC

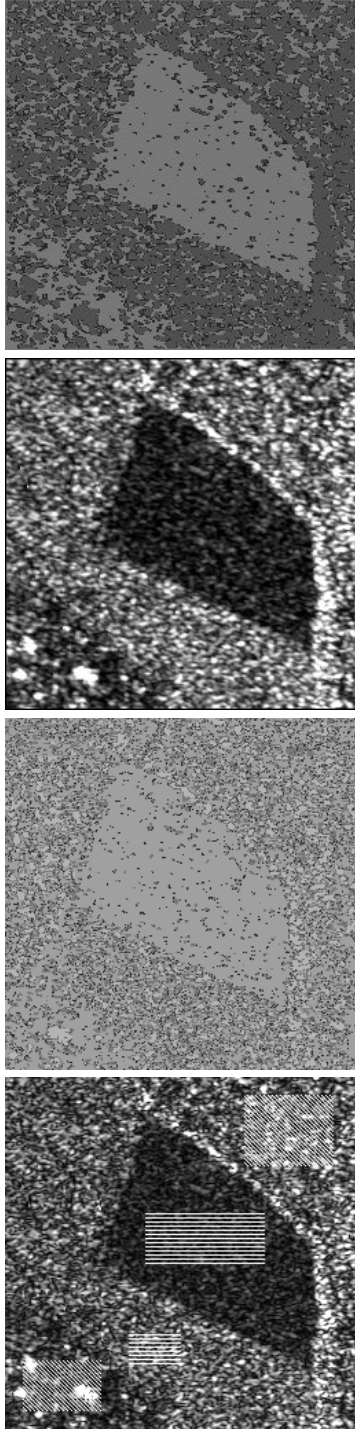


(b) One iteration and GMLC



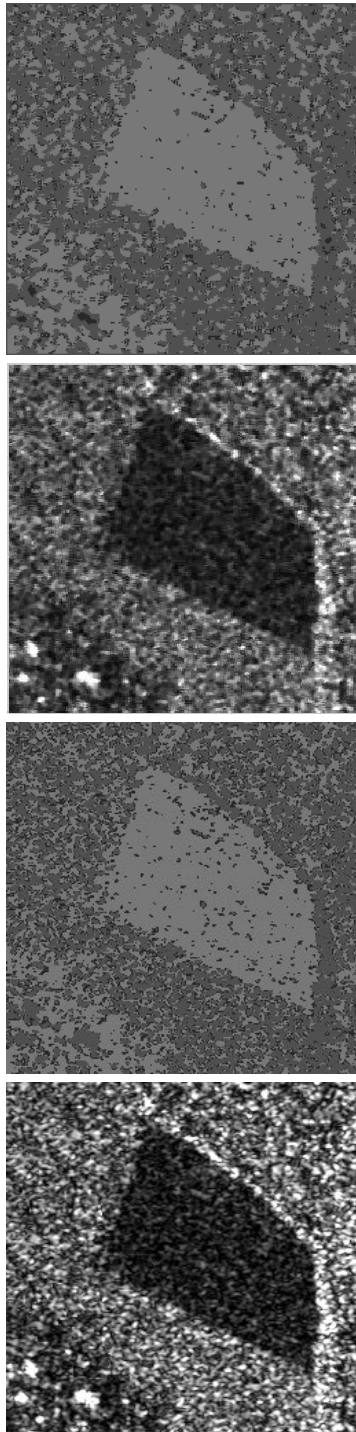
(c) 95 iterations and GMLC

Figure 2: Training by region of interest: simulated data



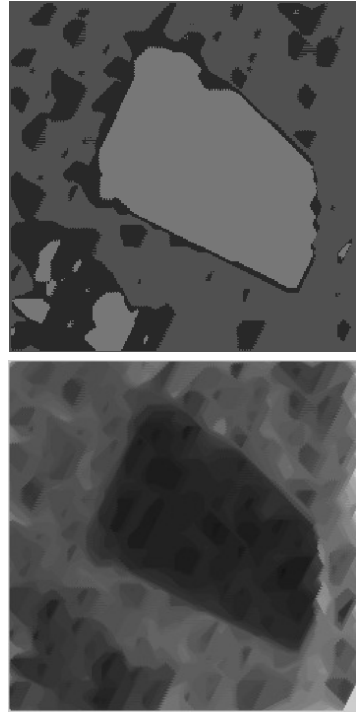
(a) Image, samples and GMLC

(b) Frost and GMLC



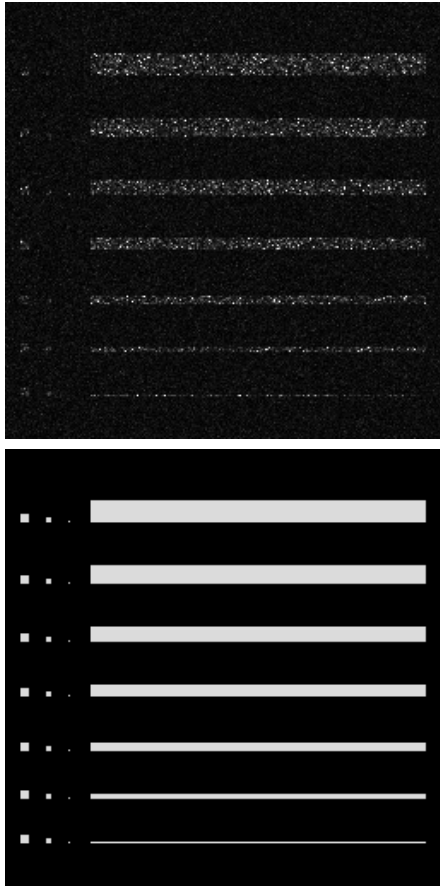
(c) Lee and GMLC

(d) Stack Filter 1 and GMLC

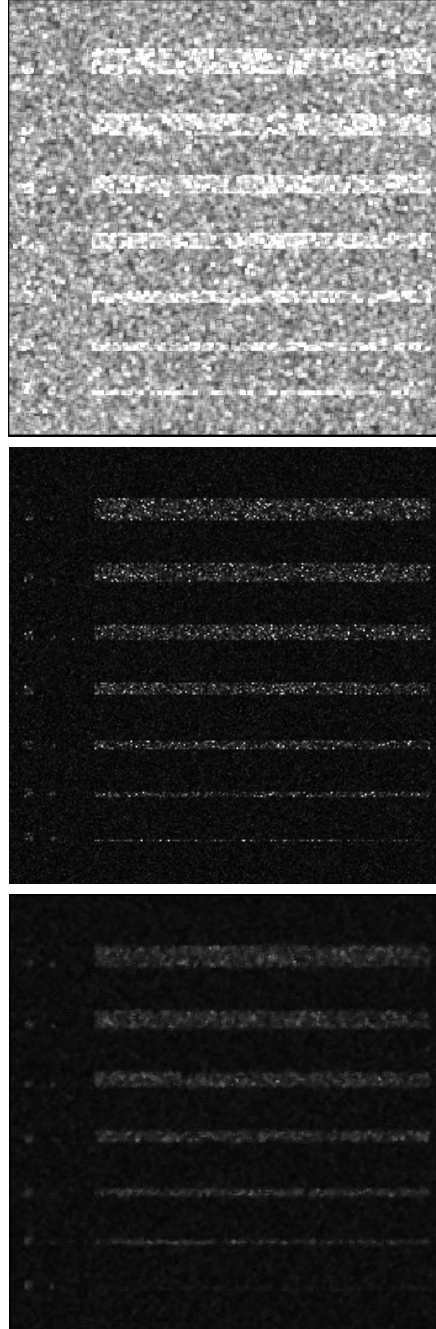


(e) Stack Filter 20 and GMLC

Figure 3: Training by region of interest: real image



(a) Phantom and simulated with $\alpha_1 = -1$ and $\alpha_2 = -5$.



(b) Stack, Lee and Frost on data with $\alpha_1 = -1$ and $\alpha_2 = -5.1-5$

Figure 4: Phantom, simulated data and Filtered with stack, Lee and Frost